In vivo retinal optical coherence tomography at 1040 nm - enhanced penetration into the choroid

A. Unterhuber, B. Považay, B. Hermann and H. Sattmann

Center of Biomedical Engineering and Physics, Christian Doppler Laboratory, Medical University Vienna, Austria

A. Chavez-Pirson

NP Photonics, UA Science & Technology Park, 9030 S. Rita Road, Tucson, AZ 85747, USA

W. Drexler

Center of Biomedical Engineering and Physics, Christian Doppler Laboratory, Medical University Vienna, Austria
wolfgang.drexler@meduniwien.ac.at

Abstract: For the first time in vivo retinal imaging has been performed with a new compact, low noise Yb-based ASE source operating in the 1 µm range (NP Photonics, λ_c = 1040 nm, $\Delta\lambda$ = 50 nm, P_{out} = 30 mW) at the dispersion minimum of water with ~7 µm axial resolution. OCT tomograms acquired at 800 nm are compared to those achieved at 1040 nm showing about 200 µm deeper penetration into the choroid below the retinal pigment epithelium. Retinal OCT at longer wavelengths significantly improves the visualization of the retinal pigment epithelium/choriocapillaris/choroid interface and superficial choroidal layers as well as reduces the scattering through turbid media and therefore might provide a better diagnosis tool for early stages of retinal pathologies such as age related macular degeneration which is accompanied by choroidal neovascularization, i.e. extensive growth of new blood vessels in the choroid and retina.

OCIS codes: (110.4500) Optical coherence tomography; (170.3880) Medical and biological imaging; (170.4470) Ophthalmology; (330.4460) Ophthalmic optics

References and links

1. D. Huang, E.A. Swanson, C.P. Lin, J.S. Schuman, W.G. Stinson, W. Chang, M.R. Hee, T. Flotte, K. Gregory, C.A. Puliafito, and J. G. Fujimoto, "Optical coherence tomography," Science **254**, 1178-81 (1991)
2. J.S. Schuman, C.A. Puliafito, and J. G. Fujimoto, "Optical coherence tomography of ocular disease," Slack Inc, Thorofare, New Jersey (2004)
3. J.G. Fujimoto, M.E Brezinski., G.J. Tearney, S.A. Boppart, B. Bouma, M.R. Hee, J.F. Southern, and E.A. Swanson," Optical biopsy and imaging using optical coherence tomography," Nature Medicine **1**, 970-2 (1995)
4. A.F. Fercher, "Optical coherence tomography," J. Biomed. Opt. **1**, 157-73 (1996)
5. W. Drexler, U. Morgner, F.X. Kärtner, C. Pitris, S.A. Boppart, X.D. Li, E.P. Ippen, and J.G. Fujimoto, "In vivo ultrahigh resolution optical coherence tomography," Opt. Lett. **24,** 1221-1223 (1999)
6. W. Drexler, U. Morgner, R.K. Ghanta, J.S. Schuman, F.X. Kärtner, and J.G. Fujimoto, " Ultrahigh-resolution ophthalmic optical coherence tomography," Nature Medicine **7**, 502-507 (2001)
7. W. Drexler, H. Sattmann, B. Hermann, T.H. Ko, M. Stur, A. Unterhuber, C. Scholda, O. Findl, M. Wirtitsch, J.G. Fujimoto, and A.F. Fercher, „ Enhanced visualization of macular pathology with the use of ultrahigh-resolution optical coherence tomography," Arch. Ophthalmol **121**, 695-706 (2003)
8. W. Drexler, "Ultrahigh resolution optical coherence tomography," J. Biomed. Opt. **9** (1), 47-74 (2004)
9. B. Považay, K. Bizheva, A. Unterhuber, B. Hermann, H. Sattmann, A.F. Fercher, W. Drexler,A. Apolonski, W.J. Wadsworth, J.C. Knight, P.S.J. Russell, M. Vetterlein, and E. Scherzer, "Submicrometer axial resolution optical coherence tomography," Opt. Lett. **27**, 1800-1803 (2002)
10. T.H. Ko, J.G. Fujimoto, J.S. Duker, L.A. Paunescu, W. Drexler, C.R. Baumal, C.A. Puliafito, E. Reichel, A.H. Rogers, and J.S. Schuman, "Comparison of ultrahigh- and standard- resolution optical coherence tomography for imaging macular hole pathology and repair," Ophthalmology **111**, 2033-2043 (2004)

#6811 - $15.00 US Received 8 March 2005; revised 14 April 2005; accepted 14 April 2005

11. E. Ergun, B. Hermann, M. Wirtitsch, A. Unterhuber, T.H. Ko, H. Sattmann, C. Scholda, J.G. Fujimoto, M. Stur, and W. Drexler, "Assessment of central visual function in Stargardt`s disease/Fundus flavimaculatus with ultrahigh-resolution optical coherence tomography," Invest. Ophthalmo. Vis. Sci. **46,** 310-316 (2005)
12. G. Wollstein, L.A. Paunescu, T.H. Ko, J. G. Fujimoto, A. Kowalevicz, I. Hartl, S. Beaton, H. Ishikawa, C. Mattox, O. Singh, J. Duker, W. Drexler , and J.S. Schuman, "Ultrahigh-resolution optical coherence tomography in glaucoma," Ophthalmology **112**, 229-237 (2005)
13. M. Hammer, A. Roggan, D. Schweitzer and G. Müller, "Optical properties of ocular fundus tissues-an in vitro study using the double-integrating-sphere technique and inverse Monte Carlo simulation", Phys. Med. Biol. **40,** 963-978 (1995)
14. American National Standards Institute,"American National Standard for Safe Use of Lasers," ANSI Z 136-1 (2000)
15. International Comission of Non-Ionizing Radiation Protection, "Revision of guidelines on limits of exposure to laser radiation of wavelengths between 400 nm and 1.4 µm," Health Phy. **79**, 432-440 (2000)
16. G. M. Hale, and M. R. Querry, "Optical constants of water in the 200 nm to 200 µm wavelength region," Appl. Opt. **12**, 555-563 (1973).
17. B. Považay, K. Bizheva, B. Hermann, A. Unterhuber, H. Sattmann, A.F. Fercher, W. Drexler, C. Schubert, P.K. Ahnelt, M. Mei, R. Holzwarth, W. Wadsworth, J. Knight, and P. Russell, "Enhanced visualization of choriodal vessels using ultrahigh resolution ophthalmic OCT at 1050 nm," Opt. Express **11**, 1980-1986 (2003)
18. A.Unterhuber, B. Hermann, H. Sattmann, W. Drexler, V. Yakovlev, G. Tempea, C. Schubert, E.M. Anger, P.K. Ahnelt, M. Stur, J.E. Morgan, A. Cowey, G. Jung, T. Le, and A.Stingl, "Compact, low-cost Ti:Al2O3 laser for in vivo ultrahigh-resolution optical coherence tomography," Opt. Lett. **28**, 905-907 (2003)
19. S.H. Yun, G.J. Tearney, B.E. Bouma, B.H. Park, and J.F. de Boer, "High-speed spectral-domain optical coherence tomography at 1.3 µm wavelength," Opt. Express **11**, 3598-604 (2003)

1. Introduction

In the last decade, optical coherence tomography (OCT) has been established as a technique for high resolution, depth resolved cross sectional imaging [1-4]. Ultrahigh resolution optical coherence tomography (UHR OCT) [5-9] is a recently developed improvement of OCT technology enabling unprecedented in vivo sub-cellular [5,8,9] as well as intraretinal visualization [6,7,8]. This novel OCT technology has been used in a clinical environment for in vivo cross-sectional imaging of macular pathologies with an axial resolution of ~ 3 µm to evaluate its clinical feasibility [7,10-12].

Since the eye is essentially transparent in the wavelength region around 800 nm, transmitting light with only minimal optical attenuation and scattering and therefore provides easy optical access to the anterior segment as well as the retina, OCT was first investigated in ophthalmology [2]. So far clinical ophthalmic OCT has been performed in the 800 nm region enabling only limited penetration beyond the retina, resulting mainly in visualizing the retina and superficial parts of the choriocapillaris/choriod. The 800 nm wavelength range was considered as an optimum to meet the imaging requirements, hence due to the availability of ultrabroad bandwidth Ti:sapphire lasers offering an unprecedented resolution of up to 3 µm in tissue as well as due to inexpensive super luminescent diodes (SLD) with low output power and bandwidth, but also low noise and lower cost, which were mainly applied in commercial available ophthalmic OCT systems. While these systems operating at a wavelength of ~ 800 nm are optimally suitable to resolve all main intraretinal layers and small morphological changes within these layers, their penetration depth is limited by the highly absorbing and scattering retinal pigment epithelium (RPE). Insufficient signal of the choroidal layers below the RPE can be retrieved at this specific wavelength.

2. Absorption and scattering in the human eye

Ocular morphology is optimally adapted to facilitate the transmittance of visible light to the retina for the purposes of absorption by the photoreceptors and following phototransduction, to initiate the process of vision. The highly scattering and absorbing melanin, the main chromophore in the RPE, acts as an absorber of excess radiation in this process and thereby reduces the penetration below the RPE significantly. The absorption of light in melanin is strongly wavelength dependant. In the 600-1200nm region it decreases monotonically with increasing wavelength while the scattering behavior of light in biological tissues shows a similar trend. It can be assumed that in vivo OCT imaging at longer wavelengths than

#6811 - $15.00 US Received 8 March 2005; revised 14 April 2005; accepted 14 April 2005

800 nm should improve the visualization of morphological features in superficial layers of the choroid. Nevertheless one limiting factor exists when going towards longer wavelengths: the human eye mainly consists of water and the water absorption increases with increasing wavelength. Thereby the signal double passing the ocular media up to the retina will be strongly attenuated. Assuming that the vitreous contains ~ 90 % water and the average human eye length is ~ 25 mm one can estimate the losses for an OCT signal at the wavelength from ~ 800 nm to about 1060 nm where the water absorption profile has a local minimum (μ_a ~ 0.015 mm^{-1} at λ = 1060 nm [13], as compared to μ_a ~ 0.0023 mm^{-1} at λ = 800 nm [13]). This results in a reduction of the detectable light signal from the retina from ~ 89.4 % at 800 nm to about 48.4 % at 1060 nm according to Fig. 1 black (maximum power density which is applicable to the eye) and green line (power density which is reflected from the internal limiting membrane). Therefore a relative sensitivity loss of 2.7 dB when imaging at 1060 nm with small bandwidth at the same power level, compared to 800 nm has to be taken into account. At an operating wavelength of 1040 nm (μ_a ~ 0.02 mm^{-1}) the reduction of the signal is even more pronounced (37.5 %) due to the stronger water absorption creating an even higher loss of sensitivity of 3.8 dB. But as depicted in Fig. 1 the power limitation of corneal exposure according to the ANSI [14](American National Standards Institute) standards as well as the similar ICNIRP-guidelines [15] (International Commission for Nonionizing Radiation Protection), is less restrictive at 1040 nm than at 800 nm. Therefore the loss might be compensated by applying more power. The diagram on the left in Fig. 1 depicts the allowed power density for collimated laser light and 10 s of continuous

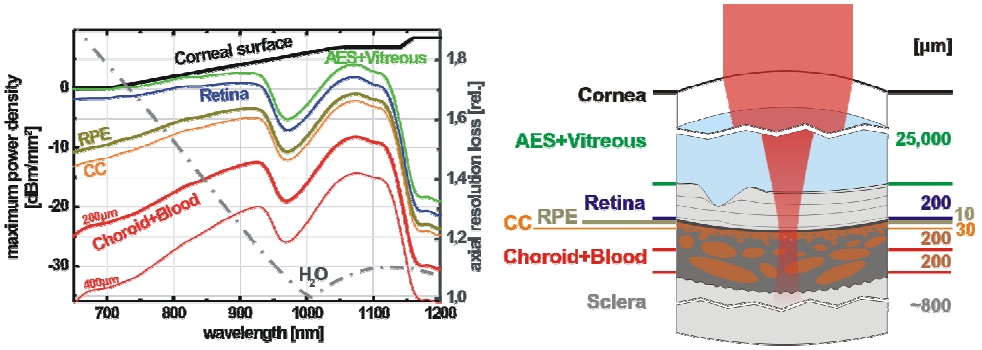

Fig. 1 Simple model of the human eye. The allowed power density for collimated laser light for 10 s continuous illumination of the cornea according to ANSI laser safety standard as well as ICRNIRP-guidelines is given in black. The green line shows the maximum power density from the front surface of the retina (internal limiting membrane) after double passing 25 mm of water of the anterior eye segment (AES) and vitreous while the blue line indicates the back surface of the photoreceptor outer segment. Water absorption mainly reduces the maximum power densities after double pass. The respective power densities from beneath the highly absorbing and scattering monocellular retinal pigment epithelium (RPE) are given in brown and from the Bruch`s membrane and choriochapillaris (CC) in orange. Representative backscattering sites inside the highly scattering choroid in a depth of 150 µm are depicted in thick red and at 300 µm in thin red. The relative spreading of the axial point spread function corresponding to a 100 nm wide spectrum at 1000 nm due to the dispersion of water corresponding to a 500 µm thick sample is shown in dash dotted grey.

illumination of the cornea according to ANSI standards or ICRNIRP-guidelines (black line). With a simple eye model (Fig. 1 right), based on experimental data of freshly excised eyes that usually resemble the material properties with less contrast than found in *in vivo* samples [13], the maximum detectable OCT power density from specific depths can be estimated (assuming a 100% reflective site). These factors would have to be multiplied by the individual reflectivities of tissue components to resemble the reflectivities found in the tomogram. The intensities are calculated for each layer (double pass) according to the data sets of absorption and scattering losses [13] based on Beer`s Law. To display the dominating effect of water absorption above 1050 nm the data sets were extrapolated over the measurement range from 1050-1200 nm with an exponential approximation, according to

#6811 - $15.00 US Received 8 March 2005; revised 14 April 2005; accepted 14 April 2005

Mie-theory, which is also found to suit well for other types of scattering tissues. After double passing 25 mm of water of the anterior eye segment (AES) and vitreous it is found that the signals coming from the retinal front surface, the internal limiting membrane (green line) and the retinal back surface below the photoreceptor outer segment layer (blue line) are mainly affected by water absorption. The respective power densities from below the RPE (brown line) with the Bruch`s membrane and choriochapillaris (CC - orange line) as well as from 200 µm (thick red line) and 400 µm (thin red line) inside the highly scattering choroid can be derived from the model and experimental data set [13] with the assumption of 70 % blood content in the choroid. In vivo OCT imaging of the human retina therefore seems only feasible at wavelengths where the absorption profile of water has a local minimum and is not severely attenuated (i.e. ~10 dB losses at 970 nm and >10 dB at wavelengths above 1130 nm between cornea and retina). But there are also convincing arguments for OCT imaging at longer wavelengths when deeper penetration is required. According to the ANSI standard or ICNIRP-guidelines, the maximum permissible light exposure in the eye increases with wavelength from ~ 1.7 mW at $\lambda \sim 800$ nm to ~ 5 mW at $\lambda \sim 1060$ nm, as calculated for 10 s continuous wave exposure. When applying the maximum allowed power on the eye of about 1.7 mW at 800 nm the OCT power signal results in 1.43 mW from the retina compared to a reduction from 4.8 mW to 1.8 mW at 1040 nm and 5 mW to 2.42 mW at 1060 nm. This results in a corresponding relative sensitivity gain of about 1 dB at 1040 nm and 2.3 dB at 1060 nm despite water absorption. This higher incident power applicable at longer wavelengths will result in an overall sensitivity improvement of ~5 dB at best as compared to the 800 nm wavelength range. It is also clearly shown in Fig. 1 that due to less scattering at longer wavelengths higher signals relative to shorter wavelengths can be obtained with increasing imaging depth. The sensitivity improvement below the RPE is 3.25 dB at 1040 nm, 7.5 dB 200 µm in the choroid and 11 dB 400 µm in the choroid.

3. Dispersion effects

An additional advantage of OCT imaging in the 1000 nm regime will also arise from the zero dispersion point of water located at ~ 1000 nm [16]. At this wavelength the OCT sample signal broadening with depth is negligible and therefore the axial resolution stays about constant over reasonable depth (grey dash-dotted line in Fig. 1). The grey line in Fig. 1 depicts the OCT signal broadening due to second order dispersion of a 500 µm thick water layer difference between sample and reference arm as a function of wavelength. It has to be noted, that although this is the major reason for axial resolution loss, absorption and higher order dispersion can adversely affect the effective resolution additionally, especially for broader bandwidth. Precisely, the latter is depicting the broadening of the correlation function if a complete compensation of dispersion is achieved at one depth, which is usually achieved by introducing a similar amount of water in the reference arm. Since eye movements limit the perfect compensation *in vivo*, the assumption of 500 µm of uncompensated material corresponds already to a well compensated measurement. The broadening of the axial point spread function in depth due to a 500 µm thick sample will be >55 % over the whole depth range at 800 nm compared to ~6 % at 1040 nm (grey dash-dotted line in Fig. 1), always taking into account that all higher order terms than second order dispersion have been neglected in this simplified model. Working close the zero dispersion point of water will therefore facilitate easier dispersion management especially with extreme myopic patients in systems without dynamic dispersion control. Consequently, sufficiently powerful broad bandwidth light sources centered at $\lambda \sim 1040$-1060 nm have great potential for ophthalmic OCT in clinical investigations. Employing light sources for ophthalmic OCT centered in the 1000-1100 nm wavelength range, might further extend the penetration depth of OCT imaging beyond the retina [17] considering the fact that the transparency of the ocular media in this region is still good. Moreover, using laser light in the 1000-1100 nm wavelength range should give less attenuation in opaque eye media, that occurs in older patients due to cataract lenses and haze in the cornea. Ophthalmic OCT imaging in the 1000-1100 nm region may find important applications such as visualizing the choriocapillaris and choroid. Early stages of

#6811 - $15.00 US Received 8 March 2005; revised 14 April 2005; accepted 14 April 2005

retinal pathologies such as age related macular degeneration (AMD) are accompanied by choroidal neovascularization, i.e., extensive growth of new blood vessels in the choroid and retina which irreversibly impairs vision in the effected regions. Therefore detection of the onset of choroidal neovascularization and periodic monitoring of its development over time can provide a valuable insight for ophthalmologists and may permit earlier and better diagnostics of retinal pathologies, as well as assignment and monitoring of a therapy at the very early stages of a disease when it is most favorably treatable. In addition, it can aid development and evaluation of novel therapeutic approaches.

4. Methods

In the present paper we demonstrate, according to our knowledge, for the first time in vivo retinal OCT in the 1040 nm wavelength range with ~ 7 µm axial resolution in tissue by employing a new compact, low noise light source based on amplified spontaneous emission (ASE, NP Photonics, λ_c = 1040 nm, $\Delta\lambda$ = 50 nm, P_{out} = 30 mW). This source is simply turn

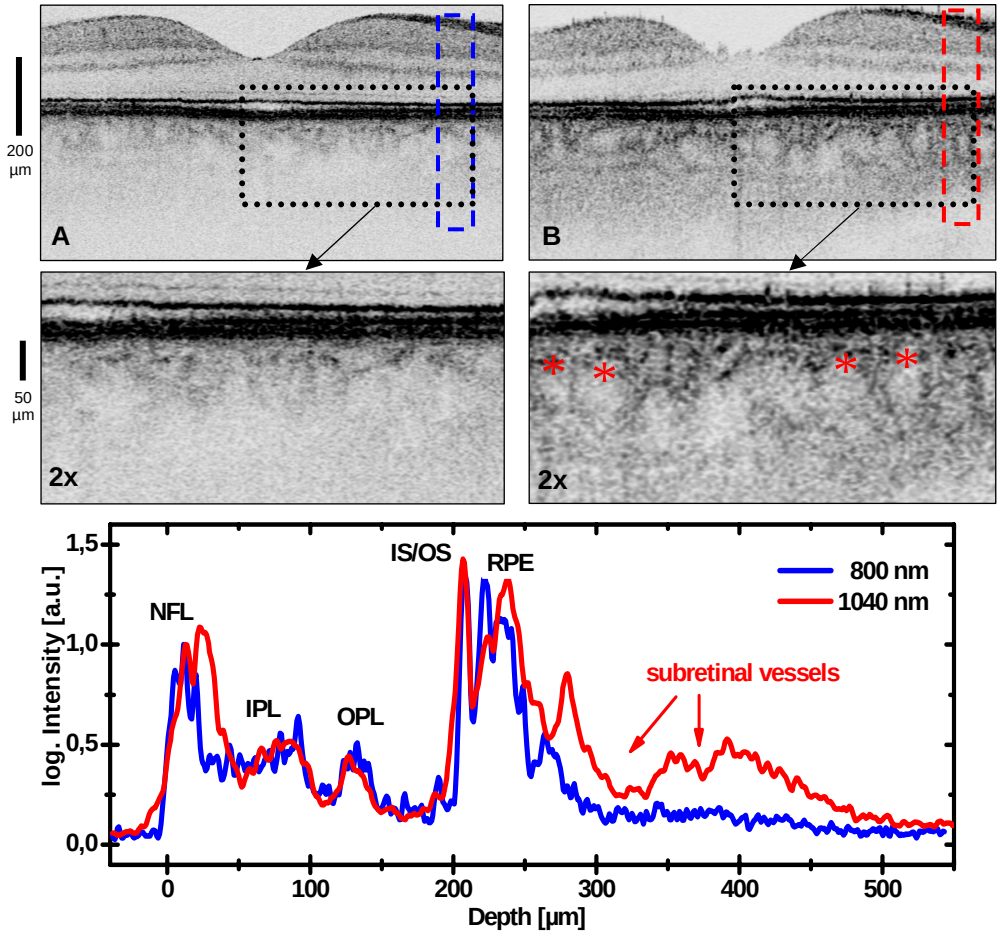

Fig. 2. Comparison of in vivo retinal OCT of the same human fovea using 800 nm (a) with 3 µm and 1040 nm (b) with 7 µm axial resolution. Both OCT systems have comparable sensitivity of ~ 95 dB. Deeper penetration into the choroid is accomplished by using 1040 nm, enabling the visualization of choroidal vessels and branching (B red asteriks) shown in two times magnification of the corresponding tomograms. Intensity diagrams obtained at 800 nm (blue curve) and 1040 nm (red curve) at similar positions depict a significant higher signal at and below the RPE at 1040 nm. A penetration depth of about 500 µm is achieved at 1040 nm in contrast to a penetration depth of about 300 µm at 800 nm.

#6811 - $15.00 US Received 8 March 2005; revised 14 April 2005; accepted 14 April 2005

key operated and therefore extremely convenient to use. It has an integrated pump laser and is microprocessor controlled. In our experimental set up this light source has been interfaced to a fiber based ophthalmic time domain OCT system [6,8] based on an OCT 2 system provided by Carl Zeiss Meditec Inc. (Dublin, California, USA) using dual balance detection with InGaAs PIN photodiodes. For easy alignment and proper fixation by the patient an aiming beam – a HeNe laser delivering approximately 5 µW onto the cornea was launched simultaneously with the ASE light source via one exit of the dual stage interferometer. In vivo measurements have been performed with up to 150 A-scans/second using 3.3 mW optical power onto the eye, well below the 5 mW maximum at $\lambda \sim 1060$ nm according to the ANSI laser safety standards as well as the ICNIRP standards for 10 s continuous wave exposure.

5. Results and discussion

Tomograms from normal human retinas are acquired at 800 nm and 1040 nm under almost the same conditions at nearly the same location. Figure 2 shows a comparison of in vivo retinal OCT imaging in the foveal region of the same healthy human subject performed with ultrahigh axial resolution (~3 µm) OCT using a compact, commercially available ultrabroad bandwidth (160 nm at full width half maximum) Ti:sapphire laser (INTEGRAL, Femtolasers Produktions GmbH, Vienna, Austria) [18] centered at 800 nm (cf. Fig. 2(a)) with the ophthalmic OCT system using the ASE light source centered at 1040 nm (cf. Fig. 2(b)) enabling ~ 7 µm axial resolution in tissue. Both OCT systems have comparable sensitivity of ~ 95 dB. All tomograms consist of 600 A-scans covering about 5-6 mm in transverse and 1-

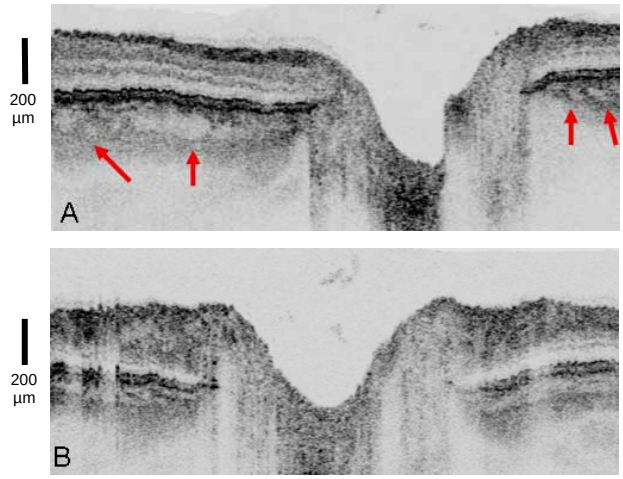

Fig. 3. Horizontal (a) and vertical (b) OCT cross-section performed with an ASE based ophthalmic OCT system centered at 1040 nm with 7 µm axial resolution. Due to enhanced penetration into the choroid several vessels are clearly visualized in the parapapillary region (arrows).

2 mm in axial direction corresponding to 600x6000 pixels. Significantly deeper penetration below the RPE into the choriocapillaris and choroid is achieved by using light with 1040 nm wavelength, clearly visualizing lacunae of choroidal vessels and branching (cf.. Fig. 2 two times magnification of the corresponding tomograms). For accurate quantitative comparison between the two wavelengths intensity profiles are also depicted. The graph shows the intensity profiles at comparable locations (red and blue dashed rectangle) averaged over 32 A-scans with comparable profile. The signals are normalized at the nerve fiber layer. It can clearly be seen that the red signal corresponding to the one obtained at 1040 nm shows deeper penetration. A subretinal vessel (red arrow) can obviously be resolved in the intensity profile at 1040 nm. The blue signal obtained from the 800 nm tomogram only shows distinguishable features down to 300 µm, i.e., ~ 80 µm into the choroid. No subretinal vessels can be seen in the intensity profile at 800 nm. Retinal imaging at 1040 nm results in an improvement of

#6811 - $15.00 US Received 8 March 2005; revised 14 April 2005; accepted 14 April 2005

penetration depth of about 200 µm. Signals down to 500 µm i.e. ~ 200 µm below the RPE can be distinguished from the noise.

Figure 3 depicts horizontal (A) and vertical (B) in vivo OCT tomograms using the ASE light source based system at 1040 nm through the optic disc of a healthy subject. Also in this case both tomograms consist of 600 A-scans covering about 5-6 mm in transverse direction and 1-2 mm in axial direction. In addition to the topography of the nerve head and intraretinal information, vessels deep below the RPE in the choroids are visualized around the optic disc.

It has to be pointed out that the contrast of the structures inside the choroid is still higher at 1040 nm, though the axial resolution is much lower. The effective axial resolution loss (cf., Fig. 1 grey dash-dotted line) at this depth has a significantly flatter slope at 1040 nm and might also be responsible for part of the improvement. This gives promise to even better visualization with higher axial resolution at deeper imaging depths in this wavelength range.

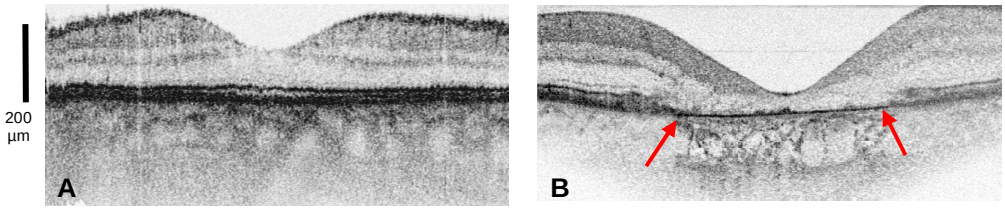

Fig. 4. Comparison of in vivo retinal OCT of a healthy human fovea at 1040 nm (a) with a human fovea with RPE atrophy (b) at 800 nm, where regions with intact RPE and defect RPE can clearly be distinguished. Only the region with defect RPE in the center indicated by the two arrows in figure B has comparable penetration at 800 nm to the tomogram acquired at 1040 nm due to reduced melanin concentration. Towards the margins at regions with intact RPE the penetration is significantly less than at 1040 nm and comparable to the tomogram acquired at 800 nm.

Comparing a normal healthy retina with intact RPE imaged at 1040 nm (cf. Fig. 4(a)) with a retina with RPE atrophy imaged at 800 nm (cf. Fig. 4(b)) indicates similar penetration depth in regions where the RPE and therefore also the melanin concentration was clearly reduced. In regions with intact RPE the penetration depth of the tomogram acquired at 800 nm was significantly smaller than at 1040 nm.

6. Conclusion

For the first time *in vivo* retinal imaging at 1040 nm with sub-10 µm axial resolution could be demonstrated using a novel, compact ASE light source in combination with a time domain ophthalmic OCT system. Compared to OCT tomograms acquired at $\lambda_c \sim 800$ nm, better visualization of superficial choroidal layers was achieved with the ASE based source ($\lambda_c = 1040$ nm). With further light source technology development, broader bandwidth light sources (~ 100-150 nm bandwidth) in the 1000-1100 nm wavelength region should enable improved axial resolution in tissue to about 2-3 µm. The low dispersion of tissue in this wavelength range should even allow helping to keep the high resolution across the whole depth, while the absorption should still remain acceptable and the scattering is significantly lower than at 800 nm. A more detailed overlap of the wavelength of the light source with the water window and therefore an adaptation of the center wavelength to about 1060-1070 nm would further increase the penetration depth. In combination of the light source with a frequency domain system fast data acquisition with 3-D imaging could be feasible [19]. This novel 1040 nm ophthalmic OCT system has great potential in clinical applications for monitoring choroidal neovascularization, associated with age-related macular degeneration. .

Acknowledgments

This work was supported in part by FWF P14218-PSY, FWF Y159-PAT, ÖNB Jubiläumsfondsprojekt 10506, the Christian Doppler Society, FEMTOLASERS Produktions GmbH, NP Photonics and CARL ZEISS Meditec, Inc. Special thanks to Peter Ahnelt for fruitful discussions concerning the eye model.

#6811 - $15.00 US Received 8 March 2005; revised 14 April 2005; accepted 14 April 2005